Anal. Bioanal. Electrochem., Vol. 17, No. 6, 2025, 461-475
https://www.doi.org/10.22034/abec.2025.725955

Analytical & Bioanalytical Electrochemistry

Full Paper

Electrochemical Detection of Rutin using Carbon Paste Electrodes Modified with Yttrium Oxide Nanoparticles

A.G. Bindu, and Ramesh S. Bhat*

Department of Chemistry, NMAM Institute of Technology, NITTE (Deemed to be University), Nitte-574110, India

*Corresponding Author, Tel.: +91-08861037310
E-Mail: rameshbhat@nitte.edu.in

Received: 26 May 2025 / Received in revised form: 25 June 2025 / Accepted: 27 June 2025 / Published online: 7 July 2025

Abstract- The current study is on the electrochemical investigation of rutin (RTN) by modifying a carbon paste electrode (CPE) using Yttrium oxide nanoparticles (Y_2O_3 NPs) and polymerization of lycine. The Y_2O_3 NPs are synthesized by yttrium (III) nitrate and urea at 350°C. The surface morphology of synthesized NPs is confirmed by Field emission scanning electron microscopy (FESEM) and the composition of NPs by energy dispersive X-ray (EDX) analysis. The modified LMYOCPE (lycine-modified yttrium oxide carbon paste electrode) exhibits remarkable electrocatalytic redox activity toward the detection of RTN in the phosphate buffer solution (PB solution) of pH 5.7. Electrochemical techniques such as electrochemical impedance spectroscopy (EIS) and cyclic voltammetry (CV) are widely employed for the investigation and evaluation of sensor performance. The fabricated electrode exhibits redox behavior for the large electroactive surface towards electron transfer. The study is novel because it combines NPs with an electrode system to create a highly sensitive, selective, repeatability, reproducibility, and stability towards RTN analysis.

Keywords- Yttrium oxide nanoparticles; Rutin; Lycine; Impedance; Cyclic voltammetry

1. INTRODUCTION

Nanoparticles have diverse development in recent eras, by their remarkable physical, chemical, morphological, and structural properties. These impactful applications across the various sector domines driving global research and innovation towards shaping the future. Yttrium oxide nanoparticles (Y_2O_3 NPs) are well-known as inorganic NPs of rare earth element

(REE) type consisting of phases like cubic, hexagonal, and monoclinic. Monoclinic are by the gas phase preparation while the other two are of chemical methods. Cubic can withstand a melting point of 2400ºC and are of chemically stable properties helps in ceramics and low temperature helps in insulator applications. They form wide band gap that helps for many applications they play an important role in many applications like ceramics, alloys, reactors, luminescence, nonlinear optics, digital communication, photochemistry, batteries, solar energy, catalytic activity, biological imagining, and semiconductor devices [1,2].

Yttrium oxide nanomaterials have been synthesized in various morphologies, including forms and different shapes likes nanorods, nests, hexagonal, and cubic structures by methods of sol-gel, precipitation, hydrothermal, plasma-assisted, microwave, green synthesis, etc. Our approach influences, related to the different means, can produce nanoparticles by simplicity, grains of nano-size with minimal impurities, and effective yield through the combustion approach for nanoparticle synthesis [3-5].

Rutin is a Vitamin P complex also known as quercetin-3-O-rutinoside belongs to flavanol glycosides in the yellow crystalline found in various forms such as vegetables, fruits, black currents, tobacco, wheat, and rose hips. It has many therapeutic benefits and with of medicinal [6,7]. Consumption above 4 g/day may affect the vitamin complex of the body and excess consumption leads to several health disorders. Different forms of analytical studies have been utilized for the detection of RTN, such as spectrophotometry, injection analysis, chemiluminescence, amperometry studies, and chromatography [8-10]. In contrast, our approach to voltammetric study demonstrates efficiency, sample preparation, standard equipment, less time investment, and budget-friendly techniques when compared to the other approaches.

Carbon-based electrodes, particularly carbon paste electrodes (GCEs), have gained prominence in electrochemical sensor development due to their affordability, extensive potential range, ease of fabrication, and outstanding electrical conductivity. Graphene is a carbon atom arranged in a hexagonal structure, that offers a wide electrochemical window, exceptional conductivity, robust chemical and mechanical stability, biocompatibility, and excellent thermal properties. BCPE plays a prominent role in low response to current in the background, quick response, swift process, cost-effective, and well-known process for low concentration detection. The investigation was based on the surface morphology and the catalytic activity towards the fabricated electrode material.

The present study introduces the combustion method for the Y_2O_3 NPs fabricated using precursor material such as Yttrium (III) nitrate and fuel as urea, confirmed by FESEM and EDX. Nanoparticles were used as a composite material for electrode modification to enhance electrochemical behavior. Through the composition method, the electrochemical behavior of RTN was improved compared to bare and nano-composite. EIS and CV techniques are employed. The electrochemical activity of RTN under varying pH, scan rates, concentrations,

interference, and simultaneous analysis. The results highlighted methods are cost-effective, stable, rapid response, high conductivity, exceptional selectivity, sensitivity, reproducibility, and repeatability.

2. EXPERIMENTAL SECTION

2.1. Chemicals and instrumentation

Yttrium (III) nitrate Hexahydrate ($Y(NO_3)_3).6H_2O$ and glycine ($C_2H_5NO_2$) were used for the preparation of nanoparticles by muffle furnace and hot air oven. The confirmation of nanoparticles morphology by FESEM and elemental composition by EDX. Electrochemical analysis was carried out through an instrument CHI-6048E from the USA of the cell containing three electrodes, where the LMYOCPE serves as the working electrode, the standard calomel electrode as the reference electrode, and the platinum wire as the auxiliary electrode. The silicon oil as a binder, carbon powder as a base material for the electrode, potassium chloride (KCl) as an electrolyte and potassium ferrocyanide($K_4Fe(CN)_6$) as an analyte. Where 0.1 M PB solution was prepared by mixing an appropriate quantity of monosodium dihydrogen phosphate (Na_2HPO_4) and disodium hydrogen phosphate (NaH_2PO_4), all chemicals were purchased from Merck, India. The chemicals were of 99% purity without additional standardization. The 25×10^{-4} M rutin, leucine solutions were prepared using double-distilled water (DW) for electrochemical analysis and was investigated using EIS, and CV. The whole experiment was carried forward at the room temperature of 30℃.

2.2. Preparation of yttrium oxide NPs

Yttrium oxide (Y_2O_3) nanoparticles (NPs) were synthesized using yttrium(III) nitrate hexahydrate as an oxidizer and urea as a fuel. Both were mixed in a stoichiometric ratio to form a homogeneous solution. The solution mixture was placed for combustion at 350°C in a muffle furnace for one hour, to form nanopowder. During combustion, the solution was transformed to a gel state further to solid by the self-propagating ignition inside the furnace by the release of gases. The formed product was thoroughly washed with ethanol and DW many times to remove the residues. Finally, the compound was dehydrated in a hot air oven at 100°C for several hours to obtain the desired yttrium oxide (Y_2O_3 NPs) nanoparticles [11].

2.3. Electrode fabrication

The fabrication of the electrode was carried out using the prepared Y_2O_3 NPs with the base material carbon powder along with the silicon oil in a 70:30 ratio and ground well until a homogenous paste mixture was formed. The formed paste was filled inside the cavity of the bare carbon paste electrode (CPE) resulting yttrium oxide carbon paste electrode (YOCPE). Thereafter, the surface of the electrode was modified by polymerization of 20 cycles using

lycine referred to as LMYOCPE (lycine-modified yttrium oxide carbon paste electrode) to carry the electroactive behavior of the study [12].

3. RESULTS AND DISCUSSION

3.1. Analysis of Y_2O_3 NPs by FESEM and EDX

The structural and morphological characteristics of Y_2O_3 nanoparticles (NPs) were clearly revealed by FESEM analysis, as depicted in Figure 1a. The analysis finds the irregular shape of the structure of grain appearance with individual particles separately. The NPs confirm the well-defined successful synthesis with the smooth texture representing the high quality and yield. The separate boundaries and space between individual nanoparticles may be due to the release of gas during the process of combustion with various and improved performance in plenty of applications. The EDX signifies the NP's composition, as reported in Figure 1b. The analysis signifies the prepared nanoparticles include 63.4% yttrium and 36.6% oxygen by weight and 24.1% yttrium and 75.8% oxygen by atomic percentage. The absence of extra peaks specifies the purity of the synthesized nanoparticles [13].

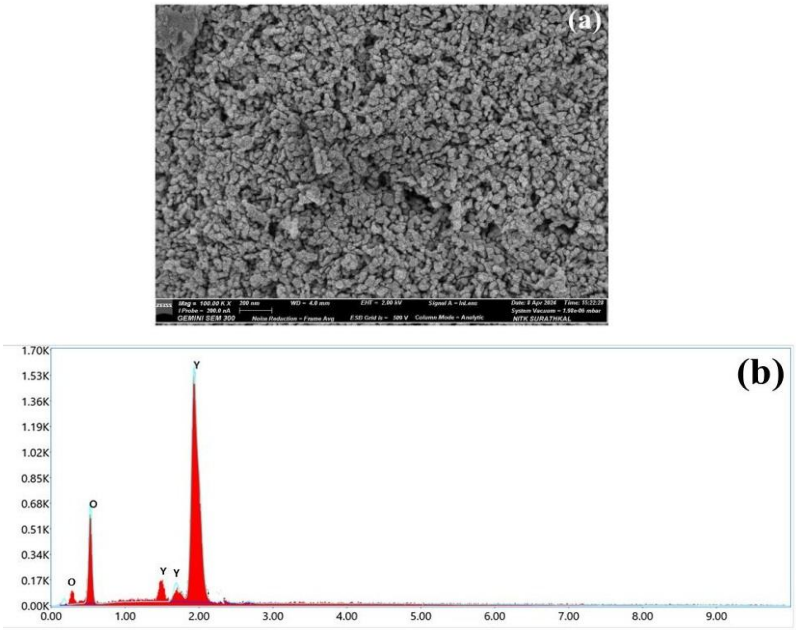

Figure 1. (a) FESEM and (b) EDX analysis of Y_2O_3 NPs

3.2. Analysis of electrochemical impedance spectra (EIS)

EIS was analyzed to estimate the charge transfer resistance (R_{ct}), solution resistance (R_s) and conductance of bare and modified electrode surfaces. This study was carried out using an electrochemical cell containing $K_4[Fe(CN)_6]$ of 1.0 mM and KCl of 0.1 M. The Nyquist plots were plotted for BCPE curve-a, and LMYOCPE curve-b are represented in Figure 2. The

higher surface area can be observed in the modified electrode resulting in the increased surface area with observed high R_{ct} and R_s with which signifies the electrode stability and additional resistance to charge transfer. The modified electrode suggests that conductivity through surface modifications with a balance between conductivity and charge transfer resistance was essential for optimizing the performance of the electrode in electrochemical activity. Bare electrodes show larger semicircles, indicating superior charge transfer capability with a lower R_{ct} value, the faster electron transfer on electrode-electrolyte interaction. The modified electrode signifies better electron mobility and surface charge transfer [14].

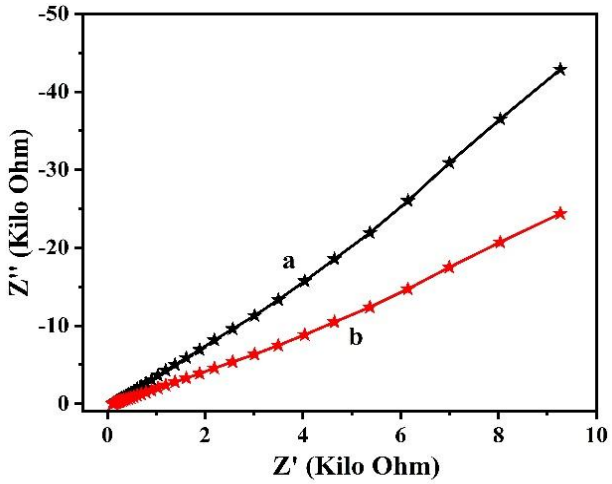

Figure 2. Nyquist plot of real current versus imaginary current for BCPE (a), and LMYOCPE (b)

3.3. Optimization of the potential gap

The potential optimization was carried out to study the RTN activity on the surface of LMYOCPE, thereby improving the selectivity and sensitivity of the peak nature.

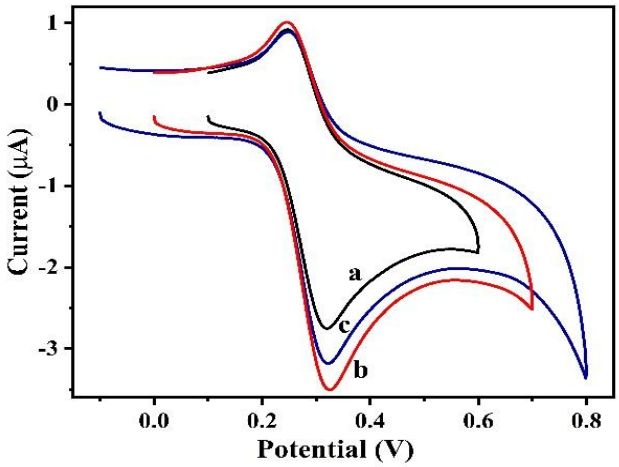

Figure 3. Optimization of potential range for 0.1 to 0.6 V (curve a), 0 to 0.7 V (curve b), and -0.1 to 0.8 V (curve c) for CV on LMYOCPE on RTN at 5.7 pH at 0.1 V/s scan rate

The potential optimization was carried out in 0.1 mM RTN in a PB solution of 0.1 M at 5.7 pH with a scan rate of 0.1 V/s was conducted using the CV technique. The peak current in the anode of RTN increased significantly when the starting E_p shifted between 0.1 V to 0.5 V. The potential was adjusted to 0 to 0.7 V, there is clear observation of a rise in Ip was noticed. Further, a decline in current was noticed as the starting E_p further varied between -0.1 to 0.8 V, and the end peak potential was fixed to a particular range of high peak current sensitivity. The starting E_p of 0 V to 0.7 V was confirmed to be the highest and maximum current response at the LMYOCPE. As a result, the particular range was considered to be optimized potential for RTN detection.

3.4. Impact of electroactive electrode surface

The electroactive surface area of BCPE (curve-a), and LMYOCPE (curve-b) was investigated by CV method using an analyte of standard solution as 1 mM $K_4[Fe(CN)_6]$ and supporting electrolyte of redox investigation as 0.1 M KCl within a potential range window of -0.3 to 0.8 V at 0.1 V/s scan rate. Figure 4 specifies the enhancement in active surface area in LMYOCPE (curve- b) than BCPE (curve a), as it was due to an increase in the peak current value by electron conductivity. The BCPE, with a lower active surface area, exhibits a weaker electrochemical response than the modified electrode, showing a higher redox peak potential (E_p) and lower redox peak current (I_p).

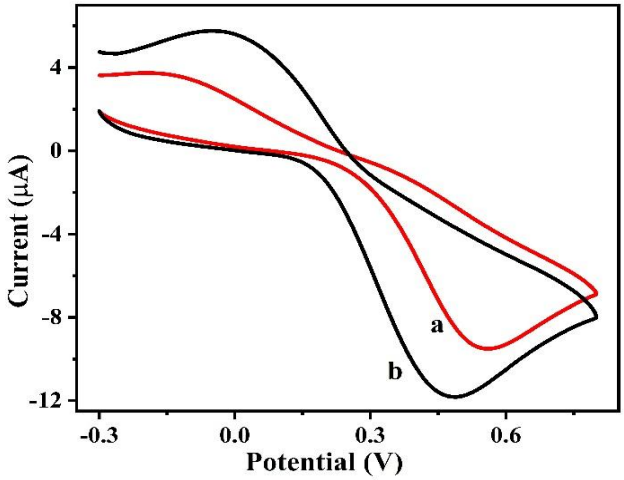

Figure 4. (a) CV for K_4 [Fe (CN)$_6$] on BCPE (a), and LMYOCPE (b) surfaces in KCl at a scan rate of 0.1 V/s

This specifies effective electrocatalytic activity sites for easy and fast transfer of electrons for high response towards RTN. The area of the active surface for LMYOCPE and BCPE of the CV curves was demonstrated using the Randles-Sevcik equation [15].

$$I_p = 2.96 \times 10^5 n^{3/2} A D^{1/2} C \upsilon^{1/2} \qquad (1)$$

I_{pa} represents the peak current, n will be the electrons involved in the reaction, A signifies the active surface area of the fabricated electrode (cm^2), D stands for the coefficient of diffusion for $K_4[Fe(CN)_6]$ (7.3×10^{-6} cm^2/s), υ give rise to the scan rate (V/s), and C will be the $K_4[Fe(CN)_6]$ (1 mM) concentration. The surface active area of BCPE was found to be 0.012 cm^2 and LMYOCPE exhibited 0.016 cm^2 of higher surface area with improved electrochemical performance for the voltammetric study.

3.5. Electrochemical behavior of RTN

The electrochemical performance of RTN was investigated by CV techniques on BCPE, YOCPE, and LMYOCPE surfaces for facilitating the redox reaction for best electrocatalytic activity as shown in Figure 5.

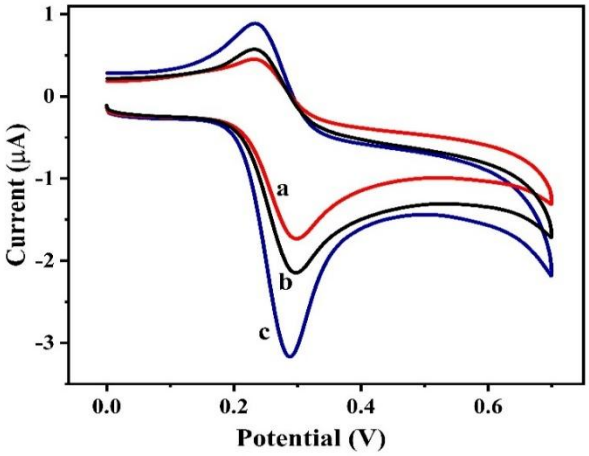

Figure 5. CV (a) for the presence (cycle c) LMYOCPE and absence (cycle b) YOCPE of 0.1 mM RTN at BCPE (cycle a) in 0.1 M PB solution of pH 5.7 at 0.1 V/s scan rate

The redox response of 0.1 mM RTN was inspected in both the absence and presence of fabricated sensor material using a 0.1 M PB solution at 5.7 pH, within 0 to 0.7 V of the potential range and 0.1 V/s scan rate. Among the tested electrodes, LMYOCPE (curve-c) exhibited the highest electrocatalytic activity, which provides the conductivity of the electrode by enhancing the peak current compared to YOCPE (curve-b) and BCPE (curve a). In the PB solution, due to the absence of RTN, there exhibits no electrochemical activity, while BCPE (curve-a) displayed the lowest response towards RTN. The response of RTN towards LMYOCPE was better in (curve b) compared to BCPE (curve a). The electrochemical polymerization of LMYOCPE helps in rapid electron transfer, quick response, sharp peaks, and high electrocatalytic activity between electrode and analyte with more active sites in the modified electrode of the quasi-reversible process of its high redox peak current (I_p) with low potential (E_p) for the electrochemical study. This modification increases redox active sites and expands the surface active area sites, thereby improving the reaction of the electrochemical

reaction behavior of RTN in CV studies. The modified electrode enhances the kinetics of the electrochemical study for more effective electrocatalytic activity.

3.6. pH effect on LMYOCPE

The concentration of hydrogen ions plays a major role in the electrochemical behavior of RTN interaction to specify the deprotonation occurrence at the particular pH range. The solution for the pH range was adjusted from 5.2 to 7.2 using 0.1 M PB solution with the RTN concentration of 0.1 mM, within a range of potential of 0 and 0.8 V at a 0.1 V/s scan rate. The redox reaction effect was analyzed in the voltammetric technique of CV through the LMYOCPE surface, in Figure 6(a).

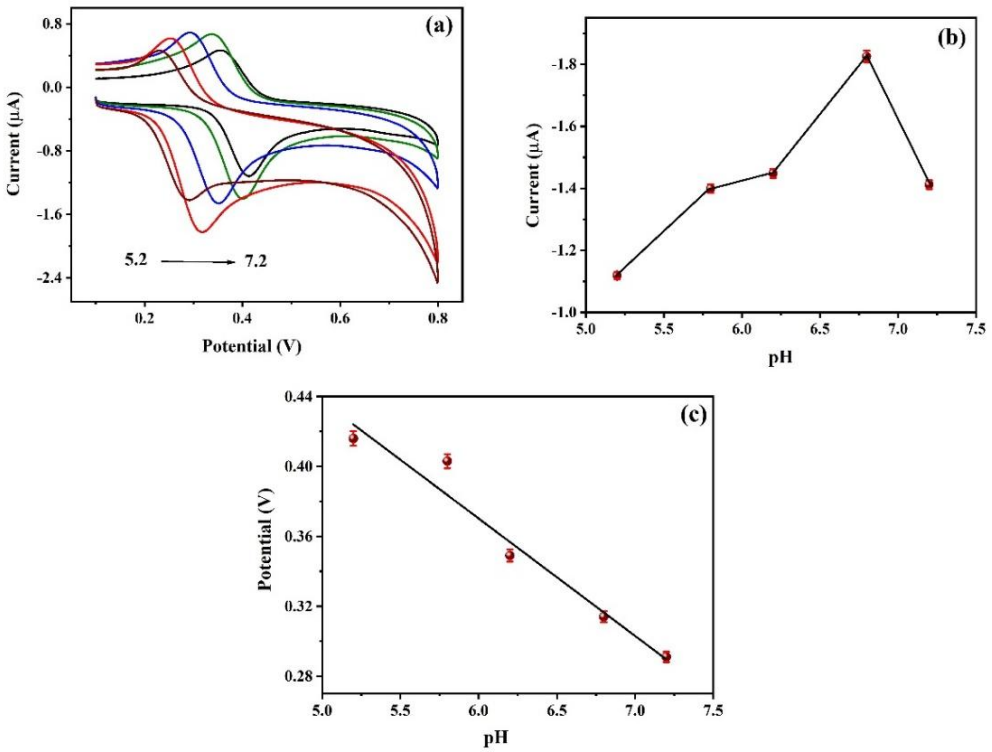

Figure 6. CV of 0.1 mM RTN in PB solution of 0.1 M on LMYOCPE surface at 0.1 V/s scan rate with change in pH from 5.2 to 7.2 (a), pH *vs.* current (b), and pH *vs.* potential (c)

The pH range increased from 5.2 to 7.2 in Figure 6(b), variations in deprotonation peak current were observed as from 5.2 to 5.7 pH there was an increase in peak current was analyzed, and at 7.2 there was a drop in the current specifies that 5.7 may be considered as optimum pH level. The E_{pa} shift toward positive potentials indicates the maximum rate of electrochemical activity at the LMYOCPE surface in Figure 6(c) of the RTN peak. The association of linear regression was represented in equations as given below [16].

$$CV: E_{pa}(V) = 0.773 - 0.067V/pH \ (R^2 = 0.965) \qquad (2)$$

Here, R^2 represents the correlation coefficient indicating good linearity and the slope of the pH *vs.* E_p of the CV is -0.067 which is close to the theoretically estimated value of -0.059 of Nernst. This specifies that almost equal numbers of electrons and protons participate in the RTN redox activity. The number of electrons was calculated using Laviron's equation was found to be 2. The optimal pH range corresponds to the point where complete deprotonation occurs, leaving no available protons observed in 5.7. Thus pH 5.7 was identified as the optimal pH corresponding to the maximum peak current for all CV analyses.

3.7. Scan rate variation of RTN on the fabricated LMYOCPE

The scan rate (SR) variation was a means for kinetic behavior, reaction mechanisms, and types of reaction in molecules on the working electrode surface for the electrochemical study at 0.1 mM RTN on LMYOCPE in PB solution of 0.1 M at pH of 5.7 was examined in Figure 7 using CV. The variation in SR from 0.020 to 0.500 V/s indicates a relative increase in peak current with increasing potential was observed, the anodic peak current (I_{pa}) shifted positively, while the cathodic peak current (I_{pc}) shifted negatively, as represented in Figure 7a.

A relationship of linearity was identified in the plots of log υ vs. log I_{pa} in Figure 7b. The slope values indicates a diffusion-controlled process for RTN on LMYOCPE. Moreover, using the slopes of E_{pa} with log υ in Figure 7c Laviron's equation helps with the calculation of electrons involved in the redox process[17].

$$B = \frac{2.303RT}{(1-\alpha)nF} \qquad (3)$$

Here R refers to the universal gas constant, α denotes the charge transfer coefficient, T will be the temperature, n signifies the electrons transferred number, and F suggests the Faraday constant. The calculated number of electrons was found to be 2, confirming the rutin mechanism of redox reaction represented in Mechanism 1.

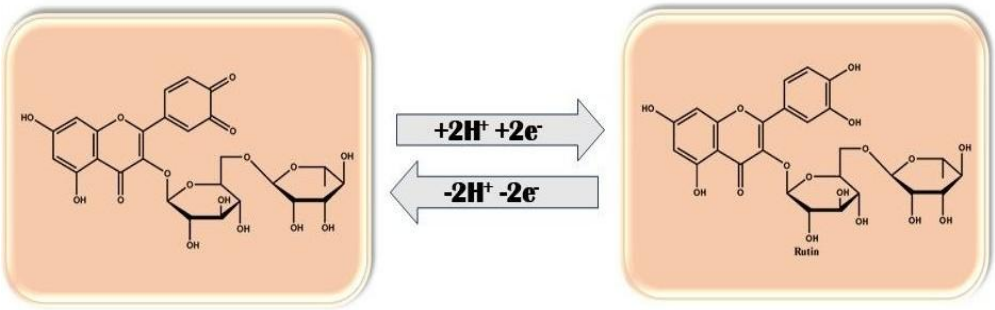

Mechanism 1. Redox behaviour of Rutin

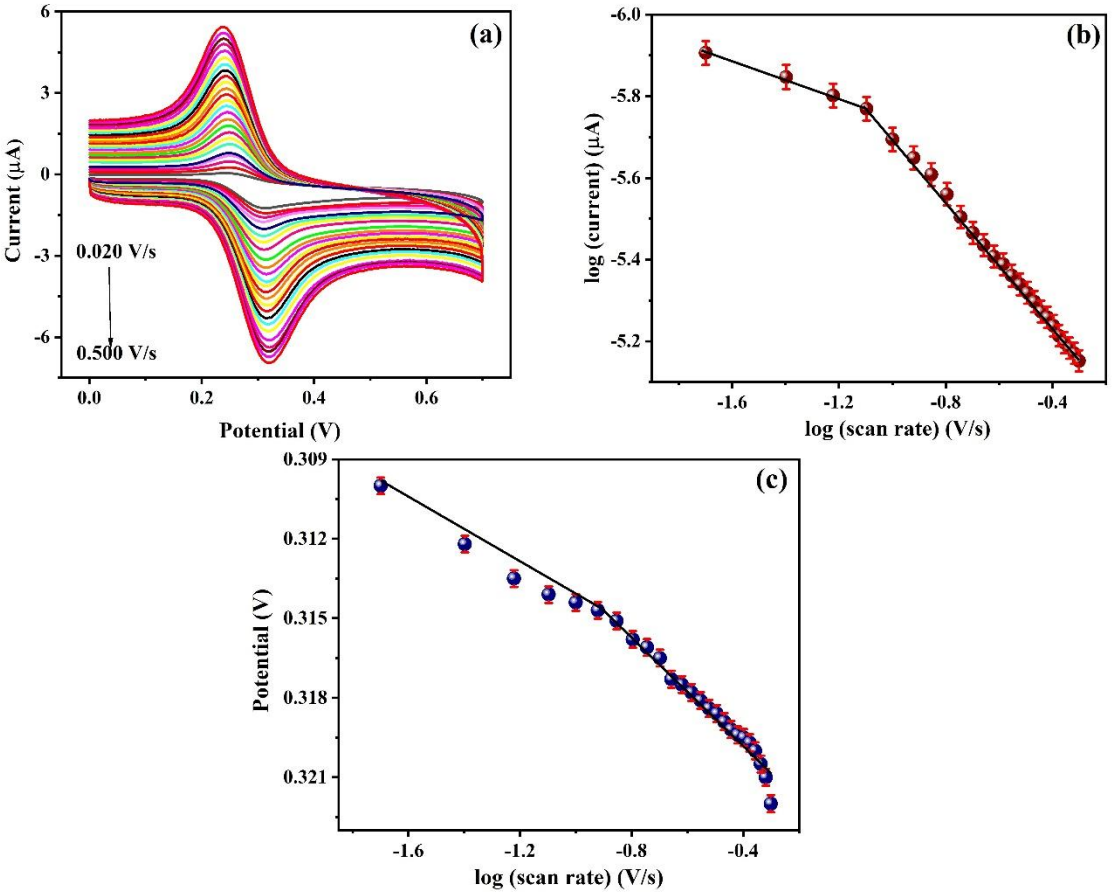

Figure 7. CV of 0.1 mM RTN in PB solution of 0.1 M on LMYOCPE surface with variation in (a) scan rate from 0.020 to 0.500 V/s, (b) log υ vs. log I_{pa}, and (c) Epa with log υ

3.8. Variation in concentration of RTN on the LMYOCPE

The sensitive detection of RTN using LMYOCPE demonstrates the electrocatalytic activities, allowing for RT identification at very low concentrations using CV in Figure 8, for the PB solution of 0.1 M within 0 to 0.7 V potential range of scan rate of 0.1 V/s. Each trial involves the step-by-step increment of 0.2 µM addition of RTN concentrations across the technique. The concentration of RTN ranged for CV from 0.010 to 0.270 µM in Figure 8(a). The increase in concentration significantly enhances the peak current, reflecting the high catalytic activity of the modified electrode, even at very low RTN concentrations, along with a strong linear correlation indicating strong electrocatalytic behavior with sharp peaks. The calibration plans of concentration of RTN *vs.* current are presented in Figure 8(b) with linear regression equations given below [18].

$$CV: I_{pa}(A) = 2.29E^{-7} + 0.001(R^2 = 0.992) \qquad (4)$$

The detection limit (DL) and quantification limit (QL) for CC were considered using the following equations:

$$\mathrm{DL} = 3 \times \frac{\mathrm{SDB}}{\mathrm{BS}} \quad (5)$$

$$\mathrm{QL} = 10 \times \frac{\mathrm{SDB}}{\mathrm{BS}} \quad (6)$$

Here, SDB signifies the standard deviation of five PB blanks for RTN, and BS indicates the RTN concentration slope vs. peak current. The calculated detection limit was 0.02 µM while the quantification limit was 0.14 µM. These results signify the high sensitivity, conductivity, selectivity, and strong electrochemical response of the developed electrode towards RTN detection in the micromolar range. A comparison table with previously reported work was noted in Table 1.

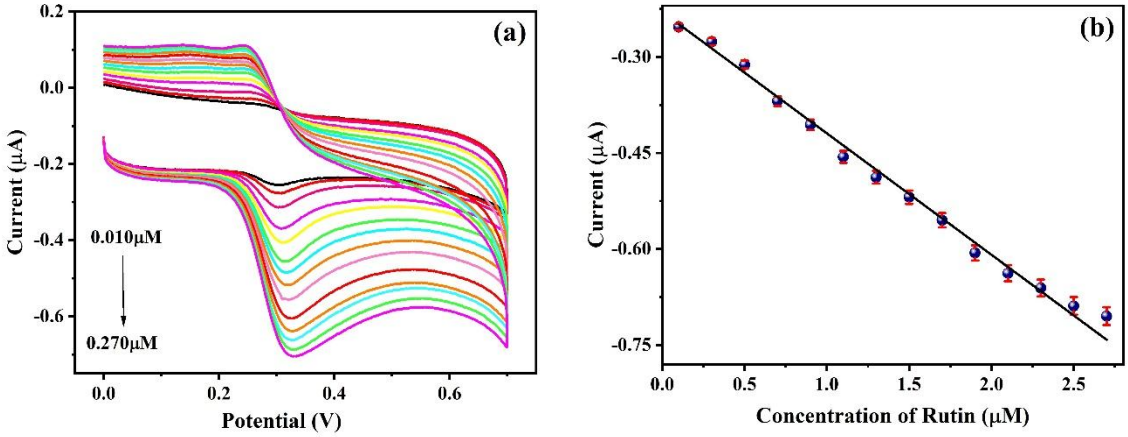

Figure 8. Concentration variation of RTN on the LMYOCPE by (a), CV from 0.010 to 0.270 µM, (b) concentration *vs.* current

Table 1. Comparison table of rutin with previously reported work

Electrodes	Range (mM)	DL (mM)	Reference
PAMGCE	0.25–10.0	0.70	[19]
CNTPE	0.19-9.9	0.30	[20]
MWCNTMGCPE	28.0-210.0	0.70	[21]
GNPPPB	0.1-6.0	0.04	[22]
PGMGPE	0.1-100	0.06	[23]
LMYOCPE	0.1-0.27	0.02	Present Work

3.9. Simultaneous analysis of RTN and HQ

The simultaneous detection of RTN and HQ (hydroquinone) was demonstrated by using CV as shown in Figure 9. The study was performed at BCPE (curve a), YOCPE (curve b), and

LMYOCPE (curve c) by 0.1M PB solution in 5.7 pH within -0.2 to 1.0 V potential range for CV, at a 0.1 V/s scan rate.

The modified LMYOCPE successfully exhibits distinct anodic oxidation peaks for RTN and HQ at 0.3 V and 0.75 V respectively, without any interference from background current. As the BCPE and YOCPE failed to reach clear peak separation for RTN and HQ. The variations in Ip and Ep significance of electrode modification in the detection process. This demonstrates that LMYOCPE provides a selective, sensitive, and advanced technique for RTN analysis in the presence of HQ. The results confirm that HQ does not interfere with RTN and has less response towards electrochemical activity, confirming the modified electrode has strong resistance to interference with other biomolecules and certifying consistent performance simultaneously.

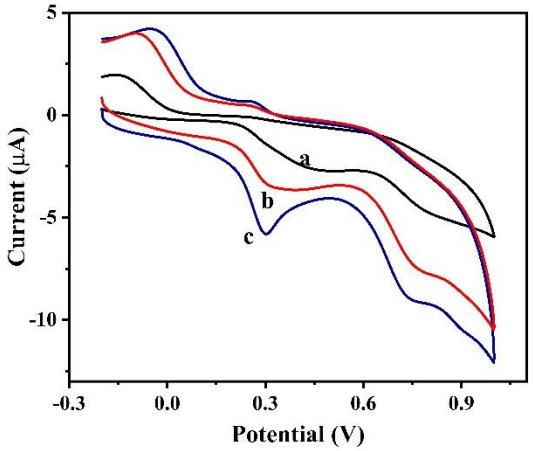

Figure 9. CV of RTN, and HQ using 0.1 M PBS of 5.7 pH on CPE (curve-a), YOCPE (curve-b), and LMYOCPE (curve-c) at 0.1 V/s scan rate

3.10. Response of interfering metals on RTN detection at LMYOCPE

The interferent analysis was examined for the selectivity of the fabricated LMYOCPE on RTN towards several interfering substances by their influence on the potential and current response. The interference study was conducted using CV techniques in 0.1M PB solution in 5.7 pH at a scan rate of 0.1 V/s to evaluate and determine the interference-free conditions for the detection of RTN as shown in Figure 10. Electrochemical analysis was performed for the metal ions and compounds including potassium (K^+), sodium (Na^+), calcium (Ca^{2+}), ascorbic acid (AA), methyl red (MR), congo red (CR), hydroquinone (HQ), as well as L-Valine (VN). The output indicates that the peak current and potential show only slight variations among these interferents by the percentage error of only ±5.0 % in I_{pa} and E_{pa}. This minimal variation, along with a standard deviation of 0.7 suggests the good interference pattern of RTN with them. These findings confirm that the fabricated LMYOCPE reveals excellent selectivity and sensitivity for RTN detection, with minimal interference from ions and other compounds suggesting that they are suitable for free from interference molecules of RTN determination.

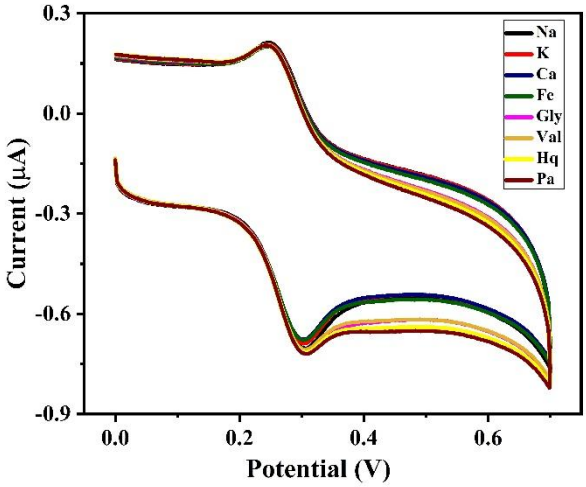

Figure 10. RTN on the LMYOCPE surface using different interferences at pH 5.7 using 0.1 V/s scan rate

3.11. Reproducibility, repeatability, selectivity, and stability of LMYOCPE

The fabricated LMYOCPE investigated the reproducibility, repeatability, and stability of RTN detection using the CV method in 0.1M PB solution at 5.7 pH within a 0 to 0.8 V range of potential at a scan rate of 0.1 V/s, as shown in Figure 11.

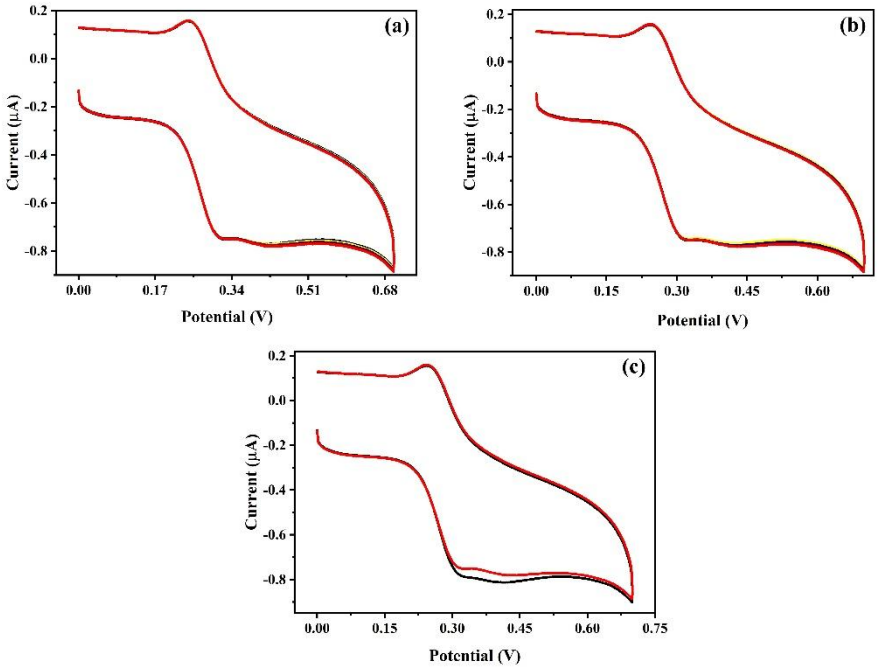

Figure 11. CV of repeatability (a), reproducibility (c), and stability (e), in 0.1 M PB solution at 5.7 pH at a scan rate of 0.1 V/s on the LMYOCPE surface

Repeatability in Figure 11(a) was measured by analyzing three different samples by the constant electrode. The found relative standard deviation (RSD) for RTN was 1.2.

Reproducibility, shown in Figure 11(b) by preparing various electrodes tested with the same sample. The RSD for RTN was found to be 1.7. The stability of the electrode was shown in Figure 11 (c) by analysis after several hours. The electrode in RTN retained itself at 96.5% confirming the long-term stability. These findings of the results collectively highlight the fabricated LMYOCPE shows outstanding repeatability, reproducibility, and stability for RTN detection.

4. CONCLUSION

The modest, eco-friendly, and cost-effective yttrium oxide NPs were prepared via the oxidizer and fuel concept combustion method, then confirmed through FESEM and EDX characterization. LMYOCPE sensor was successfully fabricated through electro-polymerization for RTN investigation. The conductivity, active surface sites, and surface electrocatalytic investigation of the fabricated sensor were successfully investigated by CV and EIS. The modified fabricated sensor exhibits a higher voltammetric peak response with maximum response towards current for RTN with a linearity range, outstanding sensitivity, selectivity, repeatability, reproducibility, and stability. In 0.1 M PB solution of 5.7 pH, achieving parameters resulting in the various pH, scan rate, concentration, simultaneous, and interference, the analysis proceeds through the kinetics of absorption reaction with the transfer of two equal protons and electrons. Further, DL of and QL for the techniques of voltammetric and fabricated sensors that were professionally applied for RTN sensing.

Declarations of interest

The authors declare no conflict of interest in this reported work.

REFERENCES

[1] C. Brecher, G.C. Wei, and W.H. Rhodes, J. Am. Ceram. Soc. 73 (1990) 1473.
[2] W. Wen, X. Yang, X. Wang, and L.G. Shu, J. Solid State Electrochem. 19 (2015) 1235.
[3] T. Andelman, S. Gordonov, G. Busto, P.V. Moghe, and R.E. Riman, Nanoscale Res. Lett. 5 (2010) 263.
[4] C. Hu, and Z. Gao, J. Mater. Sci. 41 (2006) 6126.
[5] J. Dhanaraj, R. Jagannathan, T.R. Kutty, and C.H. Lu, J. Phys. Chem. B 105 (2001) 11098.
[6] J. Zhou, K. Zhang, J. Liu, G. Song, and B. Ye, Anal. Methods 4 (2012) 1350.
[7] S. Hu, H. Zhu, S. Liu, J. Xiang, W. Sun, and L. Zhang, Microchim. Acta 178 (2012) 211.
[8] H. Xu, Y. Li, H.W. Tang, C.M. Liu, and Q.S. Wu, Anal. Lett. 43 (2010) 893.
[9] Z. Song, and S. Hou, Talanta 57 (2002) 59.

[10] D. Šatínský, K. Jägerová, L. Havlíková, and P. Solich, Food Anal. Methods 6 (2013) 1353.
[11] R.S. Bhat, J. Environ. Chem. Eng. 13 (2025) 116046.
[12] R.S. Bhat, A.G. Bindu, S. Shivani, and A.C. Hegde, Anal. Bioanal. Electrochem. 17 (2025) 204.
[13] R.S. Bhat, Appl. Chem. Eng. 7 (2024) 1.
[14] R.S. Bhat, K.B. Munjunatha, S.I. Bhat, K. Venkatakrishna, and A.C. Hegde, J. Mater. Eng. Perform. 31 (2022) 6819.
[15] A.G. Bindu, R.S. Bhat, J.G. Manjunatha, and B. Kanthappa, Inorg. Chem. Commun. 169 (2024) 113104.
[16] E. Laviron, J. Electroanal. Chem. 39 (1972) 1.
[17] A.M. Bond, F. Marken, E. Hill, R.G. Compton, and H. Hügel, J. Chem. Soc. Perkin Trans. 2 (1997) 1735.
[18] R. Shashanka, D. Chaira, and B.K. Swamy, Int. J. Sci. Eng. Res. 7 (2016) 1275.
[19] X. Chen, Z. Wang, F. Zhang, L. Zhu, Y. Li, and Y. Xia, Chem. Pharm. Bull. 58 (2010) 475.
[20] A.C. Oliveira, and L.H. Mascaro, Curr. Anal. Chem. 7 (2011) 101.
[21] G. Ziyatdinova, I. Aytuganova, A. Nizamova, M. Morozov, and H. Budnikov, Collect. Czechoslov. Chem. Commun. 76 (2012) 1619.
[22] N. Hareesha, J.G. Manjunatha, Z.A. Alothman, and M. Sillanpää, J. Electroanal. Chem. 917 (2022) 116388.
[23] B.M. Amrutha, J.G. Manjunatha, H. Nagarajappa, A.M. Tighezza, M.D. Albaqami, and M. Sillanpää, Diagnostics 12 (2022) 3113.